Eur. J. Mech. B/Fluids, **18**, (1), 3-12, 1999

Absolute inviscid instability of a ring jet with back-flow and swirl

A. MICHALKE

ABSTRACT. – The absolute instability of a ring jet with back-flow and swirl has been investigated on the basis of the inviscid linearized theory for incompressible flow. An axisymmetric disturbance mode is found to be only convectively unstable. The first azimuthal mode can become absolutely unstable, if the ring jet has a back-flow on the jet axis, and an additional swirl can increase the instability. However, for large swirl the absolute instability is suppressed. A ring jet without back-flow becomes absolutely unstable only in the presence of swirl.© Elsevier, Paris.

1. Introduction

For the flow simulation of an aero-engine combustor Lehmann *et al.* (1997) recently carried out experiments on a swirl nozzle with two concentric air streams leaving the nozzle with slightly different but equally directed swirls. LDA-measurements showed that the flow field consisted of a ring jet with back-flow along the jet axis for a maximum swirl velocity of the order of the maximum jet velocity. The back-flow velocity on the axis was about 50% of the maximum jet velocity. The measurements showed that a strong coherent velocity fluctuation of the first azimuthal mode existed close to the nozzle exit. This phenomenon suggests the possibility that an absolute instability is the cause of these fluctuations.

Similar flow fields may also be found in vortices formed above delta wings or in trailing vortices from wingtips.

Since the circular jet without swirl is unstable if viscous effects are neglected (see, for instance, Michalke (1984)), for large Reynolds numbers it is reasonable to investigate the jet flow with swirl using inviscid linearized theory as well. The disturbance equation for this case has already been given by Howard and Gupta (1962). Based on these equations, the inviscid instability of the incompressible Q-vortex has been analyzed by Leibovich (1984). Later, the inviscid compressible temporal instability of the Batchelor vortex has been investigated by Stott and Duck (1992).

The question of absolute instability in free shear flows has been adressed in the fundamental papers of Huerre and Monkewitz (1985) and (1990). According to their results, we may expect that a circular ring jet with back-flow can become absolutely unstable (see also the study of absolute instability in circular wakes by Monkewitz (1988)), but the effect of an additional swirl is not fully clarified. In a numerical study by Delbende *et al.* (1998) for the similar case of a Batchelor vortex, the introduction of a moderate amount of swirl was found to strongly promote absolute instability.

The aim of the present paper is to look for the inviscid, local absolute instability of an incompressible ring jet with back-flow and swirl. As suggested by the experiment mentioned above, the main attention is focussed on the first azimuthal disturbance. In section 2, the model for the undisturbed basic flow of a ring jet with back-flow and swirl is introduced. In section 3, the linearized, inviscid instability theory for incompressible

Hermann-Föttinger-Institut für Strömungsmechanik, Technische Universität Berlin, Sekr. HF 1, Strasse des 17. Juni 135, 10623 Berlin, Germany.
E-mail: ulf.michel@dlr.de

0997-7546/99/01/

flow is presented and the conditions for an absolute instability are discussed. Finally, in section 4, the results of the analysis are presented.

2. Basic flow in the ring jet with back-flow and swirl

The basic incompressible flow of the aero-engine combustor model used by Lehmann *et al.* (1997) is modelled by an axial velocity U and a swirl with circumferential velocity component W. In a parallel-flow approximation the radial V-component is neglected. In a cylindrical coordinate system (x, r, φ) the mean velocity vector is thus $(U(r), 0, W(r))$. The axial velocity component $U(r)$ consists of a ring jet with a possible back-flow on the jet axis with $U(0) = U_0 < 0$. The maximum jet velocity is $U_{\max}$ at $r = R$. If all velocities are normalized by $U_{\max}$, the pressure by $\rho U_{\max}^2$ and all lengths by R, we have (without introducing new notation for nondimensional quantities) $U(r)$ with $U(1) = 1$ and $U(0) = U_0 < 1$. We use a modified "Monkewitz profile" which is given by

$$U(r) = 4BF(r)[1 - BF(r)] \tag{1.1}$$

where $F(r)$ is given by Monkewitz and Sohn (1988) as:

$$F(r) = [1 + (e^{ar^2} - 1)^N]^{-1}. \tag{1.2}$$

The quantity B depends on U_0:

$$B = 0.5[1 + (1 - U_0)^{1/2}] \tag{1.3}$$

and $a(U_0)$ is determined by the condition $U(1) = 1$. $N \geq 1$ is a shape parameter that controls the thickness of the jet shear layer, i.e., the maximum of dU/dr.

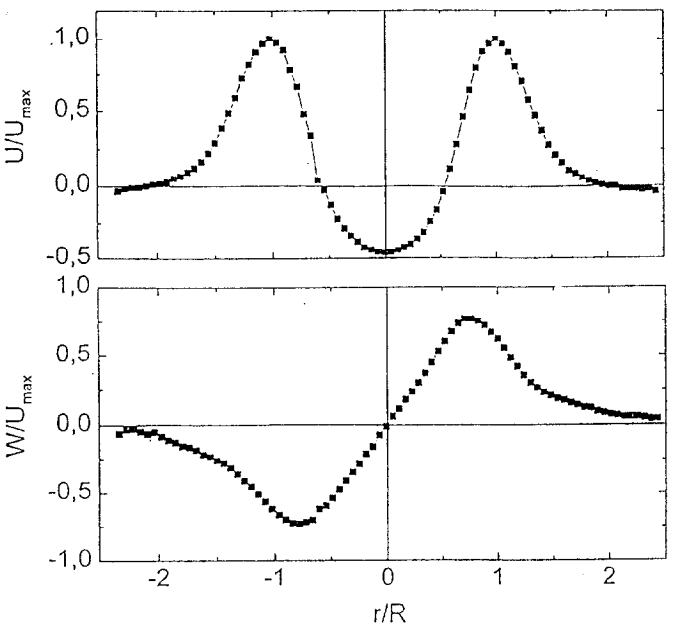

Fig. 1. – Profiles of axial velocity $U/U_{\max}$ and swirl velocity $W/U_{\max}$ vs. radial coordinate r/R in the experiments of Lehmann with the nozzle decribed by Lehmann *et al.* (1997)

The normalized swirl velocity $W(r)$ is taken as the stationary Hamel-Oseen vortex field given by:

$$W(r) = \frac{A}{r}\left[\frac{1-\exp(-br^2)}{1-\exp(-b)}\right] \tag{1.4}$$

where $A = W_{\max}/U_{\max}$ is a swirl parameter. For $b = 1.2564315$ $W(r)$ has a maximum at $r = 1$, i.e., $W(1) = A$. In practical cases, the back-flow velocity U_0 and the swirl parameter A are coupled, since the back-flow is generated by the swirl, but here we can assume the two quantities to be independent.

An example of experimental results for the axial and swirl velocity profiles at a distance of 0.8 nozzle diameters downstream of the nozzle is shown in Figure 1. The tests were carried out by Lehmann with the nozzle described by Lehmann *et al.* (1997). However, only the centre nozzle was operated so as to better simulate the current analytical model. The power-spectral density of the axial velocity fluctuations at a radial position $r/R = 1.7$ is shown in Figure 2. The peak at about 1700 Hz is due to the helical motion in the flow.

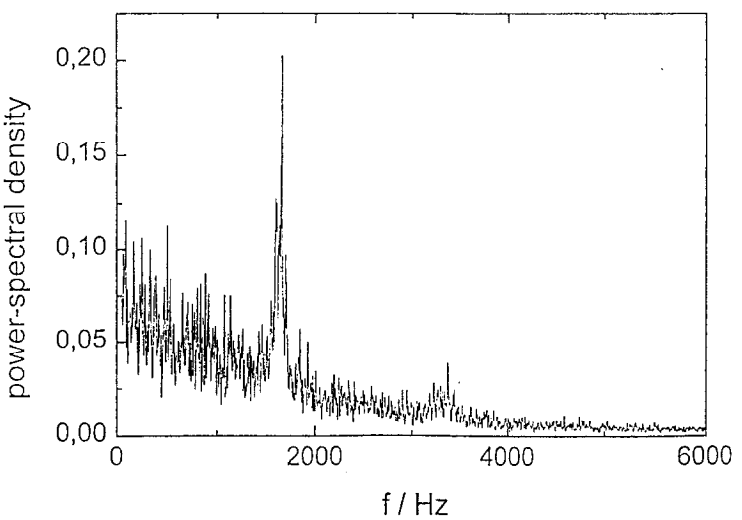

Fig. 2. – Power-spectral density of the axial velocity fluctuations at a radial position $r/R = 1.7$ for the case shown in Figure 1. The peak near 1700 Hz is due to helical motion.

In Figure 3 the ring jet velocity profile $U(r)$ according to eq. (1.1) is shown for $N = 1$ and $U_0 = 0$; -0.3; -0.5, and in Figure 4 for $N = 2$ and the same values of U_0. In Figure 5 the swirl velocity profile $W(r)$ is shown for the swirl parameter values $A = 0.2$; 0.5; and 1.0.

3. Inviscid disturbance equation and absolute instability

The inviscid disturbance equations are obtained by introducing small disturbances

$$(u', v', w', p') = (u(r), v(r), w(r), p(r))\exp(i[\alpha x + m\varphi - \omega t]) \tag{2.1}$$

into the incompressible Euler and continuity equations in cylindrical coordinates and linearizing around the given basic flow. Here α is the complex wave number and ω the complex frequency, m is the azimuthal wave number. If the u- and w- velocities are eliminated, we obtain:

$$r\sigma\frac{dp}{dr} = i[2WZ - r\sigma^2]v - \frac{2mW}{r}p \tag{2.2}$$

$$\frac{\sigma}{r}\frac{d}{dr}[rv] = i[\alpha^2 + (m/r)^2]p + \left[\alpha\frac{dU}{dr} + m\frac{Z}{r}\right]v \tag{2.3}$$

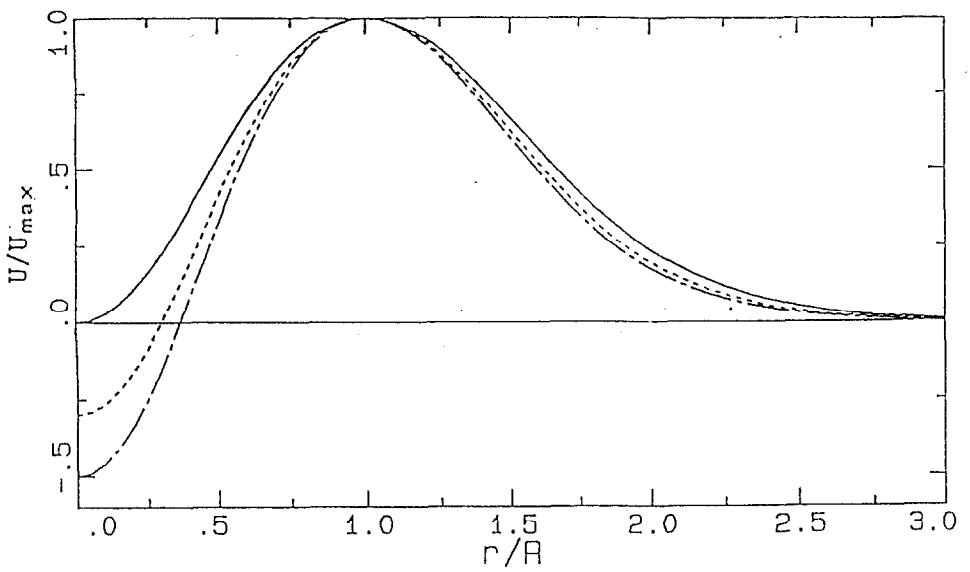

Fig. 3. – Ring jet velocity profile $U/U_{\max}$ vs. radial coordinate r/R.
Jet parameter $N = 1$; back-flow parameter $U_0 = 0$ (——); -0.3 (– – –); -0.5 (– · –).

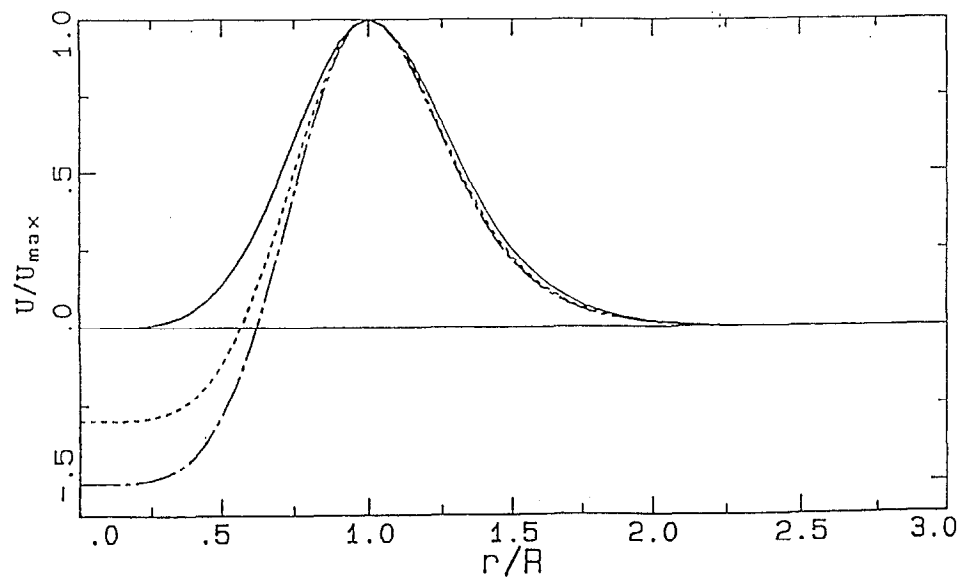

Fig. 4. – Ring jet velocity profile $U/U_{\max}$ vs. radial coordinate r/R.
Jet parameter $N = 2$; back-flow parameter $U_0 = 0$ (——); -0.3 (– – –); -0.5 (– · –).

where

$$\sigma(r) = \alpha U(r) + m\frac{W(r)}{r} - \omega \tag{2.4}$$

and $Z(r)$ is the axial vorticity component of the swirl defined by:

$$Z(r) = \frac{dW}{dr} + \frac{W}{r}. \tag{2.5}$$

If p is eliminated from (2.2) and (2.3), the Howard–Gupta equation for v is recovered.

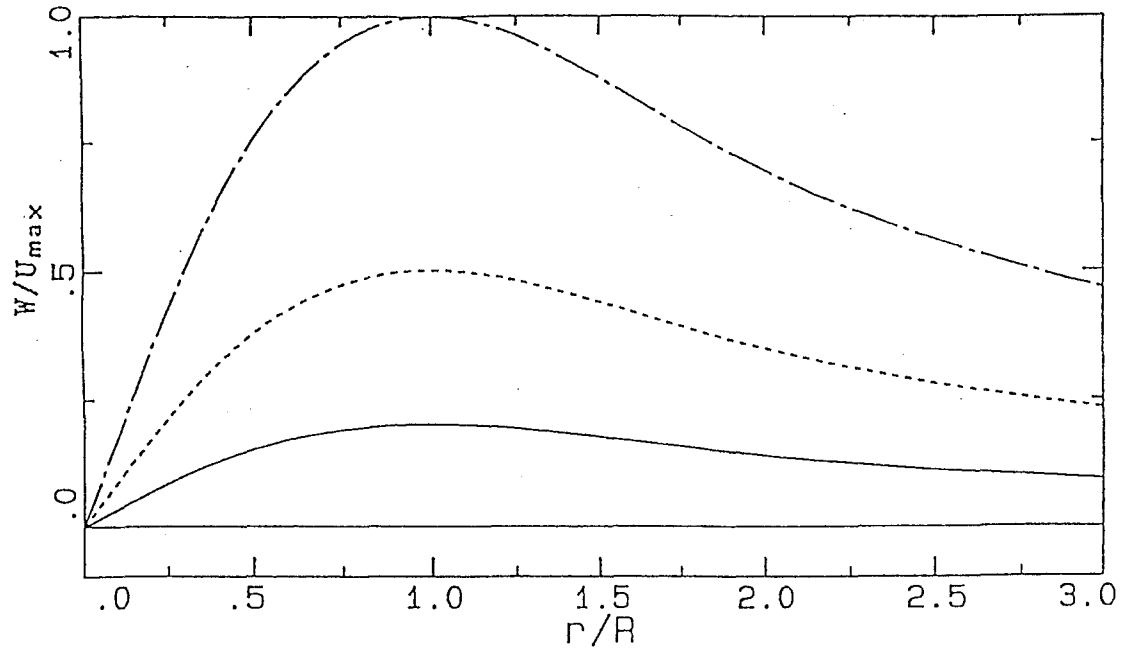

Fig. 5. – Swirl velocity profile $W/U_{\max}$ vs. radial coordinate r/R.
Swirl parameter $A = W_{\max}/U_{\max} = 0.2$ (——); 0.5 (– – –); 1.0 (– · –).

The boundary conditions require that $v(r)$ and $p(r)$ remain bounded on the jet axis $r = 0$ and that both quantities vanish for $r \to \infty$. The asymptotic behaviour for $r \to \infty$ can be obtained, if we take into account that in (1.1) and (1.4) we have U, dU/dr, $Z \to 0$, but $W/r \to A_\infty/r^2$ with $A_\infty = A/(1 - \exp(-b))$. If we substitute $\Phi = rv$, we find, following Michalke and Timme (1967), in the asymptotic limit $r \to \infty$;

$$\frac{d}{dr}\left[\frac{r}{m^2 + (\alpha r)^2}\frac{d\Phi}{dr}\right] - \Phi/r = 0 \tag{2.6}$$

with the decaying solution $\Phi = rK'_m(\alpha r)$, where K_m is the modified Bessel function of the second kind and order m. Hence, with (2.3) we find for $r \to \infty$:

$$v(r) = K'_m(\alpha r); \quad p(r) = -(i/\alpha)[mA_\infty^2/r - \omega]K_m(\alpha r) \tag{2.7}$$

where the differential equation for the modified Bessel functions has been used.

For $r \to 0$ we find from (1.1) and (1.2) $U(r) = U_0 + O(r^{2N})$; $dU/dr = O(r^{2N-1})$ and from (1.4) a rigid body rotation $W(r) = \Omega r$ with $\Omega = A_\infty b$, $Z(r) = 2\Omega$ and $\sigma \to \sigma_0 = \alpha U_0 + m\Omega - \omega$. In this limit $r \to 0$ it is more convenient to eliminate v from (2.2) and (2.3) which leads to the differential equation of the modified Bessel functions for the pressure p:

$$\frac{d^2p}{dr^2} + \frac{1}{r}\frac{dp}{dt} - [\beta^2 + (m/r)^2]p = 0 \tag{2.8}$$

where

$$\beta^2 = \alpha^2[1 - \mu^2]; \quad \mu = 2\Omega/\sigma_0 \tag{2.9}$$

As a consequence, the required bounded solution is, with (2.2):

$$p(r) = I_m(\beta r): \quad v(r) = \frac{i\alpha}{\sigma_0(1-\mu^2)^{1/2}}[I'_m(\beta r) + m\mu I_m(\beta r)/\beta r] \tag{2.10}$$

where I_m is the modified Bessel function of the first kind and order m.

The numerical solution of the eigenvalue problem is now quite simple. The system (2.2) and (2.3) is integrated by means of a Runge-Kutta-Fehlberg procedure of $O(h^8)$ starting with (2.10) at $r = 10^{-6}$ up till $r = 1$ yielding $p_1(1)$ and $v_1(1)$, and from r_∞, where the asymptotic solution (2.7) is valid, back to $r = 1$ yielding $p_2(1)$, $v_2(1)$. The eigenvalue condition then follows from the matching of these solutions at $r = 1$, requiring:

$$G(\omega, \alpha) = \frac{p_1(1)}{v_1(1)} - \frac{p_2(1)}{v_2(1)} = 0. \tag{2.11}$$

This condition leads, for given ω, to a relation $\alpha(\omega)$, or, for given α, to $\omega(\alpha)$.

Typically, for an inviscid disturbance equation like the Rayleigh equation, eigenvalues $\alpha(\omega)$ exist only up to a "neutral" frequency ω_n, since solutions always come in complex conjugate pairs. Furthermore, we can see from (2.2) and (2.3) that, if the swirl is reversed, i.e., A is replaced by $-A$, the equations remain unchanged if m is replaced by $-m$, as well. Hence we can restrict our investigation to $m \geq 0$, if positive and negative $A's$ are considered.

An absolute instability exists, accordingly to Huerre and Monkewitz (1985), if the eigenvalue relation (2.11) has a solution with zero complex group velocity, i.e., $d\omega/d\alpha = 0$ for a pair (ω_0, α_0) with $\omega_{0i} > 0$, provided that this point corresponds to the pinching of a "downstream" and an "upstream" branch. The downstream branch thereby corresponds to a spatial branch $\alpha(\omega)$, with ω_i fixed, that is located entirely in the upper half of the complex α-plane when ω_i is sufficiently large. The downstream branch is correspondingly located in the lower half of the α-plane for large ω_i. With the eigenvalue equation (2.11) we have

$$G(\omega, \alpha) = 0: \quad \frac{\partial G}{d\alpha} = \frac{\partial G}{\partial \omega}\frac{d\omega}{d\alpha} + \frac{\partial G}{\partial \alpha} = 0. \tag{2.12}$$

Hence the condition of vanishing complex group velocity $d\omega/d\alpha = 0$ is equivalent to $\partial G/\partial\alpha = 0$. Hence the conditions

$$G(\omega, \alpha) = 0; \quad \frac{\partial G(\omega, \alpha)}{\partial \alpha} = 0 \tag{2.13}$$

are necessary for absolute instability. In the present study $\partial G/\partial\alpha$ has been calculated by central differences. When a pair (ω_0, α_0) is found which satisfies both equations (2.13), it has to be checked whether this point of vanishing group velocity is generated by the pinching of a downstream and an upstream branch. This check is important, since for the present basic flow (U, W) several points with $d\omega/d\alpha = 0$ exist which do not satisfy the pinching condition. Absolute instability is then found for $\omega_{0i} > 0$, and ω_{0r} is the corresponding absolute frequency.

4. Numerical results

For the U-profile with $N = 1$, $U_0 = -0.3$ and $A = 0$ (no swirl), a vanishing group velocity $d\omega/d\alpha = 0$ for the first azimuthal mode $m = 1$ has been found for $\omega_0 = 0.5014 + i0.0510$; $\alpha_0 = 1.6964 - i0.7820$. To check the pinching condition, the curves $\alpha(\omega)$ are shown in Figure 6 in the complex α-plane for fixed values of $\omega_i = 0$

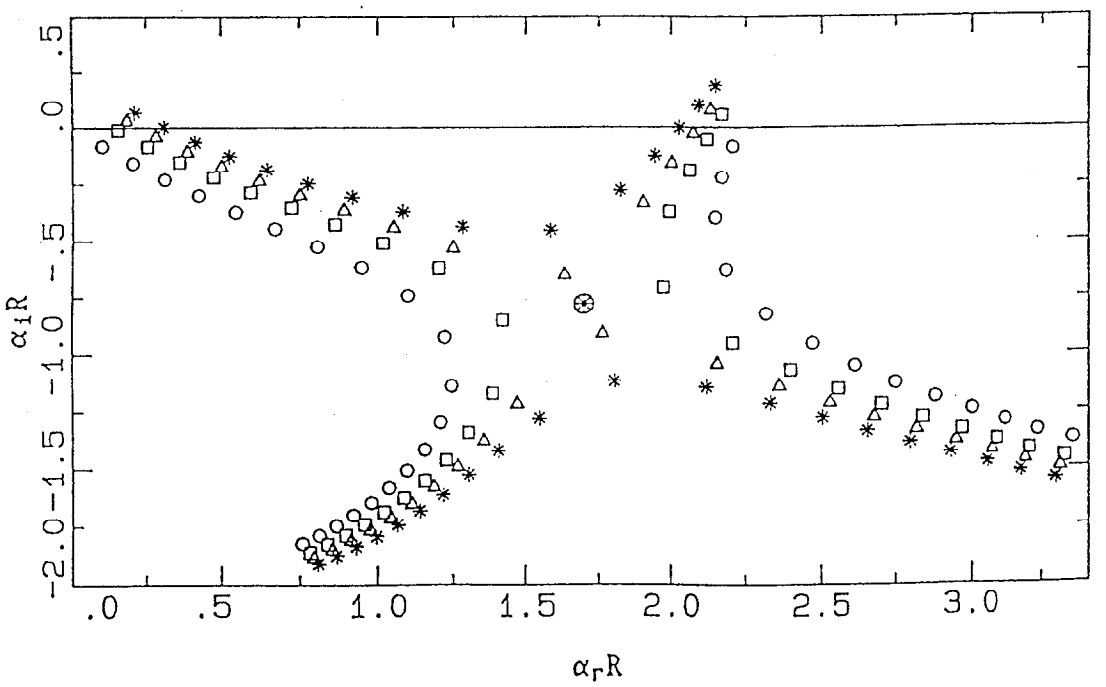

Fig. 6. – Eigenvalues α for constant $\omega_i R/U_{\max}$ around $d\omega/d\alpha = 0$ ($\otimes$) with $\omega_0 R/U_{\max} = 0.5014 + i0.0510$; $\alpha_0 R = 1.6964 - i0.7820$; ring jet profile with $N = 1$; $U_0 = -0.3$ without swirl ($A = 0$). First azimuthal mode $m = 1$; $\omega_i R/U_{\max} = 0$ (○); 0.035 (□); 0.055 (△); 0.075 (∗).

(○); 0.035 (□); 0.055 (△); 0.075 (∗). It is obvious that the pinching condition is satisfied, since the upper and lower curves move up and down, respectively, when ω_i changes from 0.055 to 0.075. For $\omega_i = 0$ and 0.035, we see the usual exchange of branches. We note that the right upper branches are not continued, since a "neutral" frequency ω_n is found. In this case, a critical layer r_c exists in the flow where $\sigma(r_c) = 0$. Here for $W(r) \equiv 0$, we have $c_{ph} = \omega_{nr}/\alpha_r = U(r_c)$; $\omega_{ni} = \alpha_i c_{ph}$, and for $\omega_r > \omega_{nr}$ no further eigenvalues exist. A simplified check of the pinching condition can also be used: Putting $\omega = \omega_0 + i\Delta\omega_i$ with $\Delta\omega_i > 0$, we should find two eigenvalues $\alpha_1 = \alpha_0 + \Delta\alpha$; $\alpha_2 = \alpha_0 - \Delta\alpha$ with $\Delta\alpha_i > 0$, and for increasing $\Delta\omega_i$, $\Delta\alpha_i$ should increase, too. It is finally noted that additional pairs (ω_0, α_0) with $d\omega/d\alpha = 0$ exist, but they do not satisfy the pinching condition.

An example where the pinching condition is not satisfied is found for the axisymmetric mode $m = 0$; $N = 1$; $U_0 = -0.3$; and $A = 0$. The results are shown in Figure 7. Here $d\omega/d\alpha = 0$ for $\omega_0 = 0.1504 + i0.0192$; $\alpha_0 = -0.7885 - i0.1705$. The curves with $\omega_i = 0.000$ (○); 0.010 (□); 0.014 (△); 0.025 (∗) exist in the lower part Figure 7, but the curves end again in the upper part at the "neutral" frequencies. Hence, the simplified check gives an eigenvalue $\alpha_2 = \alpha_0 - \Delta\alpha$, but an eigenvalue $\alpha_1 = \alpha_0 + \Delta\alpha$ does not exist. As already mentioned, the condition $d\omega/d\alpha = 0$ is also satisfied for ω_0^*, α_0^*. It is noted that preliminary results for *viscous* instability show that the pinching condition is satisfied for ω_0^*, α_0^*, since damped eigenvalues exist for $\omega_r > \omega_{nr}$ but the absolute growth rate is found to be negative. A more detailed analysis of the viscous absolute instability would be the next step.

The absolute instability for a given azimuthal mode with mode number m in the inviscid case can be characterized by the temporal growth rate $\omega_{0i} > 0$, and the corresponding frequency ω_{0r}, which depend on the basic flow quantities: swirl parameter A, back-flow parameter U_0, and the jet parameter N. For the axisymmetric mode with $m = 0$, no absolute instability was found in the parameter range investigated. In the following, we restrict our attention to the first azimuthal mode $m = 1$, which was observed in the experiment.

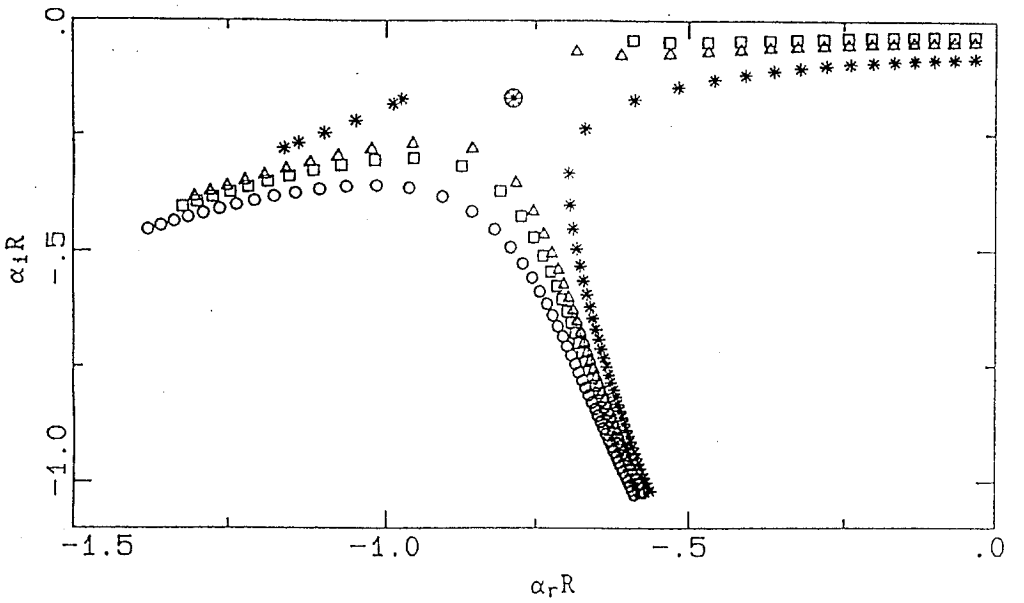

Fig. 7. – Eigenvalues α for constant $\omega_i R/U_{\max}$ around $d\omega/d\alpha = 0$ ($\oplus$) with $\omega_0 R/U_{\max} = 0.1504 + 0.0192$; $\alpha_0 R = 0.7885 - i0.1705$; ring jet profile with $N = 1$; $U_0 = -0.3$ without swirl ($A = 0$). Axisymmetric mode $m = 0$; $\omega_i R/U_{\max} = 0.000$ (○); 0.010 (□); 0.014 (△); 0.025 (∗).

In Figure 8, ω_{0i} and ω_{0r} are shown for $m = 1$ as a function of the swirl parameter $A = W_{\max}/U_{\max}$ for different back-flow parameters $U_0 = 0$; -0.3, -0.5 and the shape parameter $N = 1$. We see that absolute instability $\omega_{0i} > 0$ exists for the ring jet without swirl ($A = 0$) if back-flow ($U_0 < 0$) is present. Adding swirl with $A > 0$ increases the absolute growth rate ω_{0i} over a finite range of A starting at $A < 0$ for $U_0 = -0.3$ and -0.5 with a maximum of ω_{0i} around $A = 0.5$ and a subsequent decrease of ω_{0i} which becomes zero for A in the range of 0.8 to 1.0. For the flow without back-flow ($U_0 = 0$), the swirl $A > 0$ leads to an absolute instability. The corresponding frequencies ω_{0r} have a minimum between $A = 0$ and 0.25 and decrease with decreasing $U_0 < 0$. From the experimental data of Lehmann *et al.* (1997) taken close to the swirl nozzle, it follows that $R = 0.78$ cm, $U_{\max} = 72$ m/s; $U_0 \approx 0.5$; $A \approx -0.7$ to 1.0. From Figure 8 it follows that in this case the dimensionless frequency is $\omega_{0r} \approx 0.78$ leading to a frequency $f \approx 1140$ Hz which has to be compared with a frequency $f \approx 1700$ Hz in the experiment. However, the measured profile $U(r)$ is different from (1.1) with $N = 1$, and is, partially, better approximated by the profile with $N = 2$, shown in Figure 4. The results for this profile with $N = 2$ are shown in Figure 9. In this case the absolutely unstable region extends to lower values of $A < 0$ for $U_0 = -0.3$ and -0.5, and the frequency ω_{0r} for $A \to 1$ is larger compared to that for $N = 1$ (see Figure 7). From Figure 9 we find for $U_0 = -0.5$ and $A = 0.8$; 0.9; 1.0 $\omega_{0r} = 0.96$; 1.26; 1.58, respectively, which correspond to dimensional frequencies of $f = 1410$ Hz; 1851 Hz; 2321 Hz. These frequencies are in the same range as the measured frequency of $f = 1700$ Hz. However, we have to remember that the swirl velocity distribution $W(r)$ given by (1.4) which has an additional concentric stream with higher swirl is rather different from the experiment.

The comparison between the calculated values of ω_{0r} and the measured frequencies presented here can only be indicative. According to the theoretical analysis of Monkewitz *et al.* (1993), the global resonance frequency is given by a saddle point criterion for ω_0, which is more stringent than that the value of ω_{0r} satisfying $\omega_{0i} > 0$ at some axial station within the flow.

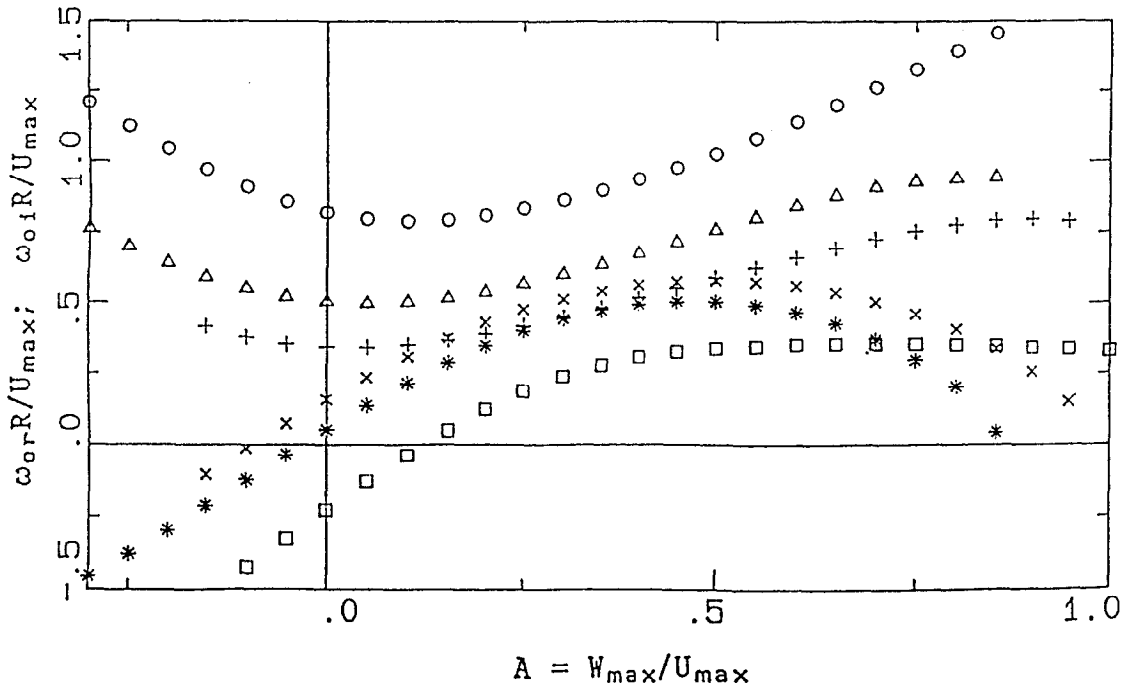

Fig. 8. – Complex frequency $\omega_0 R/U_{\max}$ of absolute instability vs. swirl parameter A for ring jet profile with $N = 1$; First azimuthal mode $m = 1$; frequency $\omega_{0r} R/U_{\max}$ for back-flow parameter $U_0 = 0$ (○); -0.3 (△); -0.5 (+); temporal growth rate $\omega_{0i} R/U_{\max}$ for $U_0 = 0$ (□); -0.3 (∗); -0.5 (×).

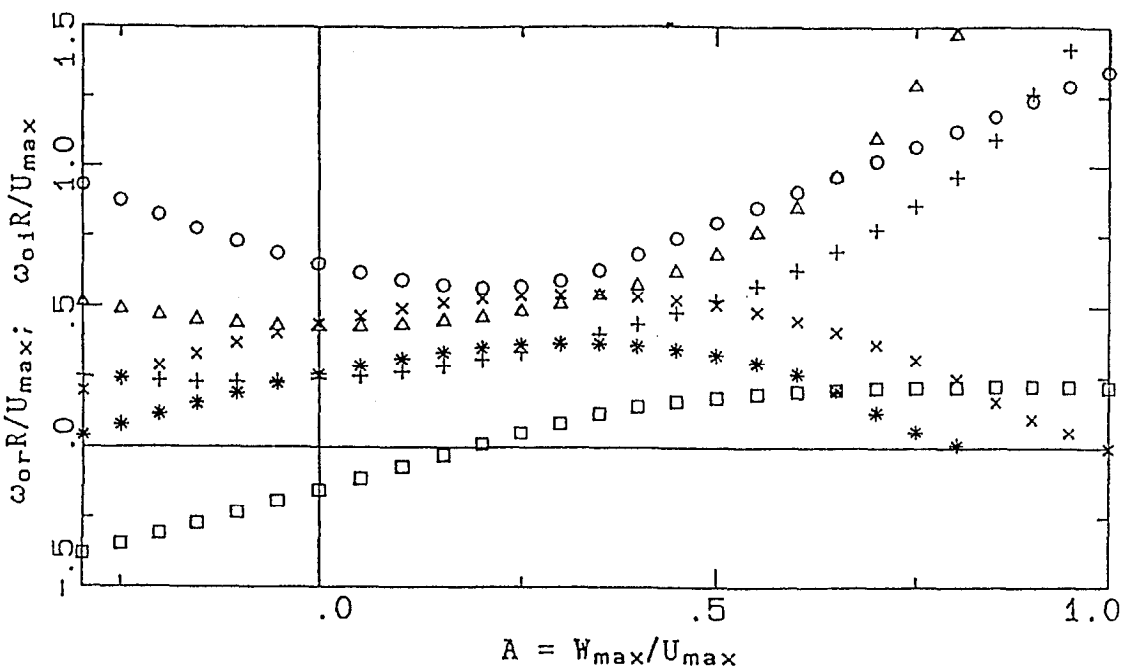

Fig. 9. – Complex frequency $\omega_0 R/U_{\max}$ of absolute instability vs. swirl parameter A for ring jet profile with $N = 2$; First azimuthal mode $m = 1$; frequency $\omega_{0r} R/U_{\max}$ for back-flow parameter $U_0 = 0$ (○); -0.3 (△); -0.5 (+); temporal growth rate $\omega_{0i} R/U_{\max}$ for $U_0 = 0$ (□); -0.3 (∗); -0.5 (×).

5. Conclusion

The flow behind a swirl nozzle used in aero-engine combustors (see Lehmann *et al.* (1997)) has been modelled by a ring jet with back-flow and swirl. The linearized, inviscid disturbance equations have been solved numerically with the aim of searching for absolute instability. The basic flow depends on a back-flow parameter U_0, a jet parameter N and a swirl parameter A. The necessary condition of absolute instability, $d\omega/d\alpha = 0$, was satisfied for several pairs (ω_0, α_0), but the sufficient pinching condition of the downstream and the upstream branch was in most cases not satisfied. Hence, for the axisymmetric disturbance with $m = 0$, no absolute instability was found for the parameters considered. However, an absolute instability exists for the first azimuthal mode with $m = 1$. Without back-flow ($U_0 = 0$), a swirl with $A > 0$ leads to absolute instability, whereas with back-flow ($U_0 < 0$) this is true even without swirl ($A = 0$). For increasing swirl with $A > 0$, the absolute growth rate is increased up to a maximum at $A \approx 0.5$, but decreases beyond this value to reach zero at $A \approx 0.8$ to 1.0. Negative swirl $A < 0$ decreases the temporal growth rate. The corresponding frequencies have a minimum in the range $A \approx 0$ to 0.25, and decrease with increasing back-flow parameter U_0. Increasing the jet shape parameter N, which corresponds to increased gradients $|dU/dr|$, expands the unstable region to lower values $A < 0$, while the absolute frequencies increase for $A \to 1$. These results support the hypothesis that the strong helical fluctuating motion experimentally found in the flow near swirl nozzles of aero-engine combustors could be related to an absolute instability of the flow. The results also indicate that the absolute instability of the ring jet with back-flow ($U_0 < 0$) can be suppressed, if the swirl is increased ($A > 1$). The present results may also be important for vortex-type flows.

Acknowledgement

The author wishes to express his gratitude to Ulf Michel, Berlin, for the suggestion of this investigation, and to Klaus Neemann, Berlin, for many fruitful discussions.

The editor thanks the reviewers Peter A. Monkewitz and Patrick Huerre for their contributions, Bernhard Lehmann for providing Figures 1 and 2, and Ulf Michel for editing the paper after the death of Alfons Michalke.

REFERENCES

DELBENDE L., CHOMAZ J.-M., HUERRE P., 1998, Absolute/convective instabilities in the Batchelor vortex: a numerical study of the linear impulse response, *J. Fluid Mech.*, **355**, 229–254.

HOWARD L.N., GUPTA A.S., 1962, On the hydrodynamic and hydromagnetic stability of swirling flows, *J. Fluid Mech.*, **14**, 463–476.

HUERRE P., MONKEWITZ P.A., 1985, Absolute and convective instabilities in free shear layers, *J. Fluid Mech.*, **159**, 151–168.

HUERRE P., MONKEWITZ P.A., 1990, Local and global instabilities in spatially-developing flows, *Ann. Rev. Fluid Mech.*, **22**, 473–537.

LEIBOVICH S., 1984, Vortex stability and breakdown: survey and extension, *AIAA J.*, **22**, 1192–1206.

LEHMANN B., HASSA C., HELBIG J., 1997, Three-Component Laser-Doppler measurements of the Confined Model Flow behind a Swirl Nozzle. In: *Developments in Laser Techniques and Fluid Mechanics*, ed.: R.J. Adrian, D.F.G. Durão, F. Durst, M.V. Heitor, M. Maeda, J.H. Whitelaw, Springer, Berlin, pp. 383–398.

MICHALKE A., 1984, Survey on jet instability theory, *Progr. Aerospace Sci.*, **21**, 159–199.

MICHALKE A., TIMME A., 1967, On the inviscid instability of certain two-dimensional vortex-type flows, *J. Fluid Mech.*, **29**, 647–666.

MONKEWITZ P.A., 1988, A note on vortex shedding from axisymmetric bluff bodies, *J. Fluid Mech.*, **192**, 561–575.

MONKEWITZ P.A., SOHN K.D., 1988, Absolute instability in hot jets, *AIAA J.*, **26**, 911–916.

MONKEWITZ P.A., HUERRE P., CHOMAZ J.-M., 1993, Global linear instability analysis of weakly non-parallel shear flows, *J. Fluid Mech.*, **251**, 1–20.

STOTT J.A.K., DUCK P.W., 1992, *The stability of a trailing-line vortex in compressible flow*, Institute for Computer Applications in Science and Engineering, NASA Langley, ICASE Report No. 92–65.

(Received 8 August 1997;
revised 30 June 1998;
accepted 6 July 1998.)